

# XMASS 1.5: The next step in Kamioka, Japan

## Benda Xu for XMASS Collaboration

Kavli IPMU (WPI), UTIAS, The University of Tokyo, Kashiwa, Chiba 277-8583, Japan

E-mail: [benda.xu@ipmu.jp](mailto:benda.xu@ipmu.jp)

**Abstract.** The XMASS program at Kamioka Observatory uses self-shielding liquid xenon scintillation detectors to search for dark matter, double beta decay, and ultimately low energy solar neutrinos. For the next stage in this program, we envision building a 1 t fiducial volume detector: XMASS 1.5. The upgraded detector design reflects our experience with the current XMASS detector. The new design requires PMTs that can intercept light traveling parallel to the inner detector surface. The first batch of these new PMTs has passed the performance verification test.

## 1. XMASS Project: Multi-Purpose Liquid Xenon Detectors

Xenon is an ideal medium for searching rare events [1–4]. Liquid xenon’s high density provides for self-shielding against external  $\gamma$  rays; its only intrinsic background comes from  $^{136}\text{Xe}$  that undergoes double-beta decay. At the Kamioka Observatory in Japan, the XMASS (Xenon detector for weakly interacting **MASS**ive particles) project uses liquid xenon scintillation to detect dark matter, double beta decay and solar neutrinos [5]. From the earliest prototypes, key technologies were developed to realize the low background (Kr  $<2.7$  ppt and Rn  $8.2 \pm 0.5$  mBq) and low-energy-threshold (0.3 keV) detector XMASS-I [6], with which WIMPs [7–9], annual modulation of dark matter [10], solar axions [11] and double electron capture [12] were searched for.

## 2. XMASS-1.5: The Next Step – Bigger and Cleaner

Recent results from particle physics have rendered the once dominant dark matter (DM) candidate, the lightest SUSY particle, less appealing. A multitude of DM candidates should be explored. Utilizing its low energy threshold, XMASS-1.5 proposes to use 5 t xenon with a 1 t fiducial volume, targeting a  $\sim 1/10$  reduction in radioactivity and a background level of  $1 \times 10^{-6}$  dru (differential rate unit, /keV/kg/day) compared to solar neutrino coherent scattering that gives  $8 \times 10^{-6}$  dru. It is expected to achieve  $1 \times 10^{-46} \text{ cm}^2$  cross section sensitivity at 100 GeV WIMP mass. The homogeneous nature of XMASS makes scaling up the detector design straight-forward. In XMASS-I, the xenon scintillation light was detected with 642 inward facing photomultipliers (PMT) mounted in pure copper. The new detector incorporates a PMT design that can intercept light parallel to the detector surface (Fig. 1), to identify and reject events originating from radioisotopes (RI) on the detector inner surface.

## 3. New PMT: R13111

Jointly developed by Hamamatsu Photonics and the XMASS Collaboration, the new 3 inch *R13111* PMT has a dome-shaped round photocathode (Fig. 1c). Its 2 inch predecessor



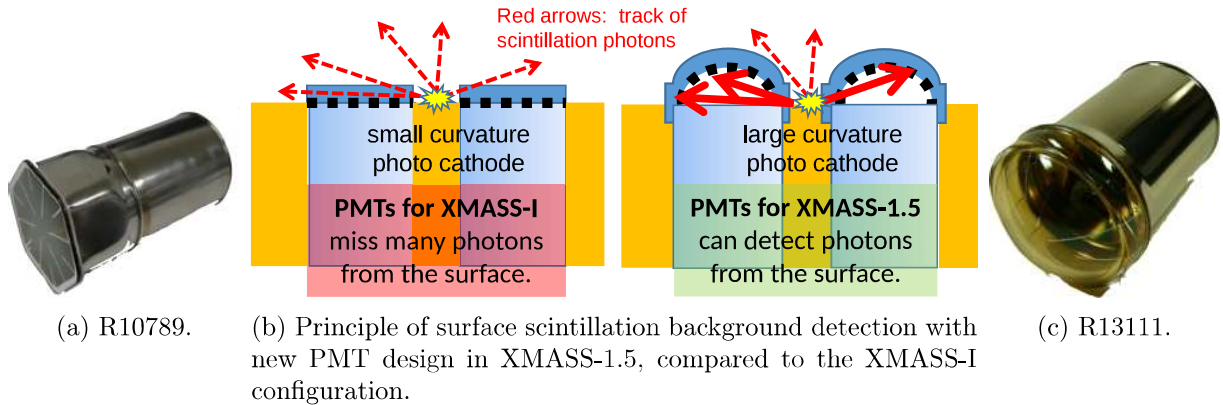
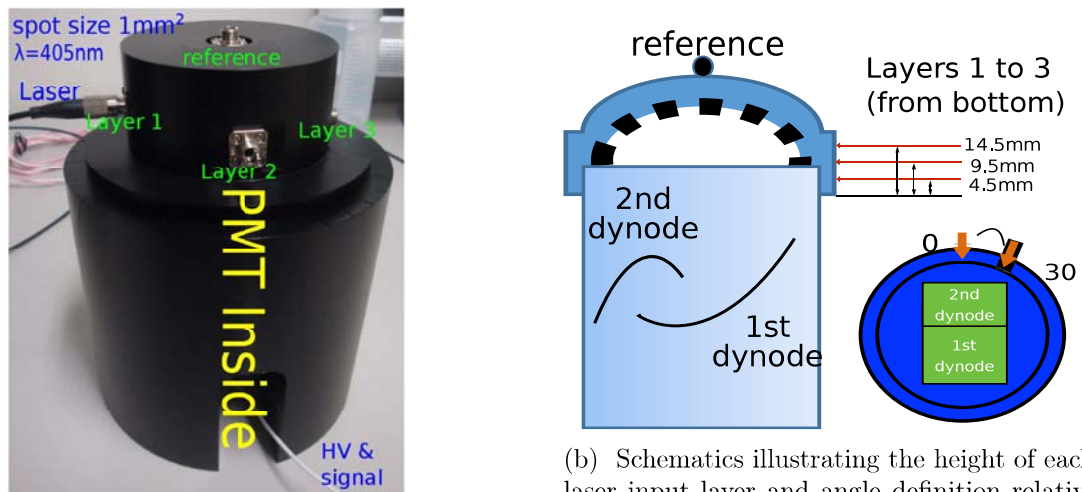


Figure 1: New PMT design. (b) shows schematics of PMTs mounted in copper holders (solid yellow); dotted black lines represent photocathodes; blue solids above the photocathodes represent the quartz windows; Solid photon arrows intercept photocathodes, allowing for detection.



(a) Photo for PMT testing jig setup showing laser input layers, high-voltage power supply and signal readout.

(b) Schematics illustrating the height of each jig laser input layer and angle definition relative to the dynodes. The left cartoon provides a side view, and the right one provides a top view in which the angle is defined clockwise.

Figure 2: The PMT test was carried out in a jig. It could direct laser light to the top of a PMT or points around a PMT axis in 3 layers.

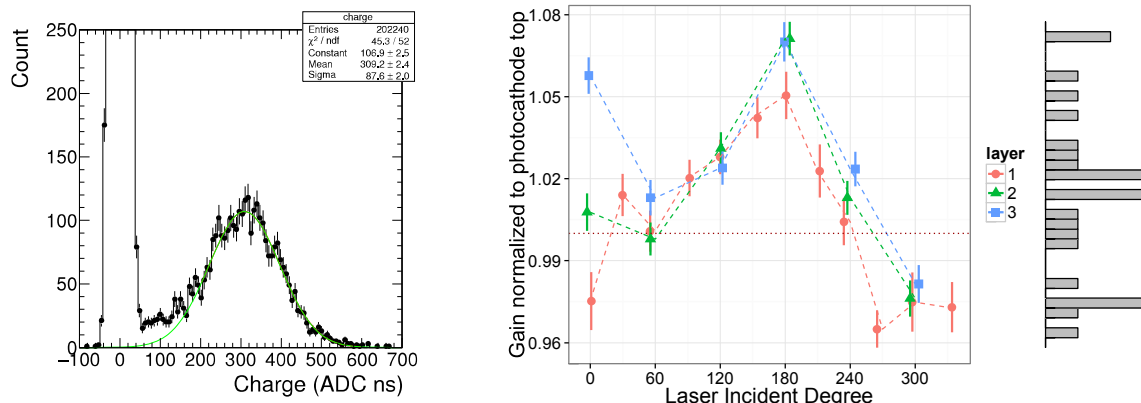
*R10789* (Fig. 1a) used in the present XMASS-I has a flat hexagonal photocathode.

A batch of *R13111* has been manufactured and delivered to Kamioka. To confirm the ability of the new PMTs to detect photons arriving parallel to the inner detector surface, they were tested in the laboratory.

### 3.1. Experimental Setup

In order to evaluate photon detection at the side of the photocathode, a jig was designed (Fig. 2a) to illuminate spots for evaluation. Its rotatable lid had light inputs to the top of a PMT and points in 3 layers at 14.5 mm (Layer 1), 9.5 mm (Layer 2) and 4.5 mm (Layer 3) from the bottom of the photocathode (Fig. 2b). The light input shone a 1 mm<sup>2</sup> spot on the photocathode.

A NIM Scientex 405 nm laser diode module was used as light source. A NIM pulse generator



(a) Charge distribution of PMT single PEs fitted with a Gaussian. (b) Variation of gain for different light input positions on the photocathode. Layer definition is in Fig. 2.

Figure 3: Single photoelectron response of R13111 at a gain of  $1 \times 10^7$ . In (b), the color and point shape represent different layers; the points and errorbars are results of Gaussian fits as in (a) and are normalized to the central value of the top input (represented by the horizontal dotted line); the dashed lines connects the points in each layer; the horizontal coordinates of the points and errorbars are slightly offset to avoid overlap.

drove both the NIM laser and CAEN V1751 flash-ADC (FADC) at 1 kHz.

The light was injected in the jig via an optical fiber. An attenuator was installed in between, because PMT is light sensitive while the laser needed to operate at high intensity to maintain stability. The attenuator consisted of a lens diverging the light beam and an aperture at a distance, shielded. Alternatively, a variable optical attenuator was used.

A CAEN V1751 FADC recorded both the 1 kHz clock pulse and the PMT waveform at 1 Gs/s. The PMT waveform was later offset to the rising edge of the clock pulse to minimize the impact of clock jitter. In addition, a Tektronix MSO 4054 oscilloscope monitored the clock and PMT output for quick inspection.

The PMTs were powered with a high-voltage power supply (HV) at the  $1 \times 10^7$  reference gain voltages supplied by the manufacturer (1500 V to 1800 V). During the test the PMT jig was shielded from external light. For each PMT, at least 30 min idle time was allocated between powering up the HV and acquiring data, in order to settle its photocathode activated by the environmental light.

### 3.2. Single Photoelectron Gain

XMASS is designed to have a low energy threshold of  $\sim 0.3$  keV, or  $\sim 4$  PMT hits. The ability to resolve a single photoelectron (PE) is crucial to the experiment. The laser output intensity and the attenuator were tuned so that the PMT occupancy (i.e. hit ratio) was  $\sim 3\%$ , to have a clear single PE peak while keeping the fraction of double PE events negligible. A waveform of a PMT was integrated after subtracting the baseline. The baseline was estimated in a time window preceding the integrating domain in the same waveform. The raw integration result is proportional to the PMT gain, with the coefficient depending on the amplifiers involved. A typical single PE peak is shown in Fig. 3a.

The new R13111 PMT was designed to detect photon from the side. In a running experiment the gain variation depending on incident photon position should be as low as possible. To measure such variation, the lid of the jig (Fig. 2) was rotated manually in  $30^\circ$  or  $60^\circ$  steps. To understand how the dynodes' geometry affect the gain, and to compare among PMTs, rotation

angle  $0^\circ$  was defined when the laser shone from the direction of the 2nd dynode (Fig. 2b).

At each angle,  $\sim 2 \times 10^4$  waveforms were collected. The gain value was extracted from a fit to the single PE peak as in Fig. 3a. The top input had optimal geometry and served as reference. The rest of the gains measured with input on photocathode sides (Layers 1,2,3) were normalized to the reference. Figure 3b shows a typical variation of gains in a single PMT. Layer 3 has the most variation, because it is the furthest from the top and is most affected by its unfavorable geometry relative to the 1st dynode. (Fig. 2b)

The overall gain variation was low enough (Fig. 3b,  $-5\%$  to  $+7\%$ ), much less than the spread of the single PE peak (Fig. 3a). The marginal histogram in (Fig. 3b) shows no structure, indicating the photocathode-dynode geometry dominated the gain variation.

### 3.3. Collection Efficiency

Collection efficiency (CE) is the probability a PE would reach the 1st dynode. In the single PE case, CE manifests itself in the occupancy. When the light intensity is way beyond the single PE, CE is reflected in the charge of the PMT output. In either case, collection efficiency (CE) is coupled with quantum efficiency (QE) which is the probability a photon induces a PE on the photocathode.

Like for gain, the geometry is the dominant factor influencing CE. In order to detect photons from the side of the PMT, CE at the photocathode side should not be low. In the single PE (Section 3.2) test, the occupancy was low to avoid double PE. While in a CE test, the statistics would be low and take a long time ( $\sim 2$  h) for each layer. The variation of laser intensity would complicate the matter. Therefore a higher light intensity was used.

The laser source and the attenuator were tuned so that each waveform contained  $\sim 5$  PEs. They were tuned at least 1 h before data acquisition, and were kept the same across the top reference and layers. Each PMT was measured in less than 1 h.

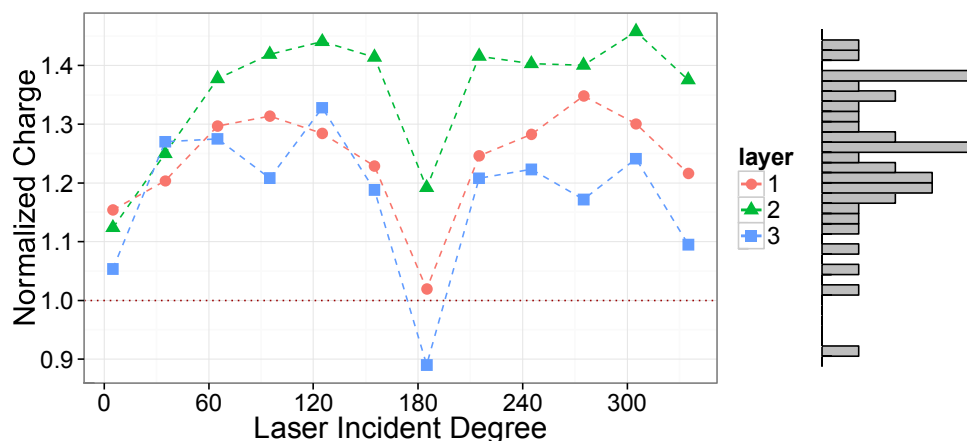


Figure 4: Charge variation. The points are from the output of Gaussian fits normalized to the central value of that of photocathode top. Other properties of the figure are the same as Fig. 3b.

The measured charge was fitted with a Gaussian. The central values are shown in Fig. 4 with negligible statistical uncertainty. The plot shows that the side of the photocathode of R13111 can detect photons, therefore transverse light to the detector surface can be collected by this kind of new PMTs.

The variation is expected from the geometric alignment of first dynode (Fig. 2b), although the range  $-10\%$  to  $+50\%$  is larger than that of gain (Fig. 3b,  $-5\%$  to  $+7\%$ ). The variance will affect energy resolution of events from the detector surface, where a precise measurement of energy is not a priority.

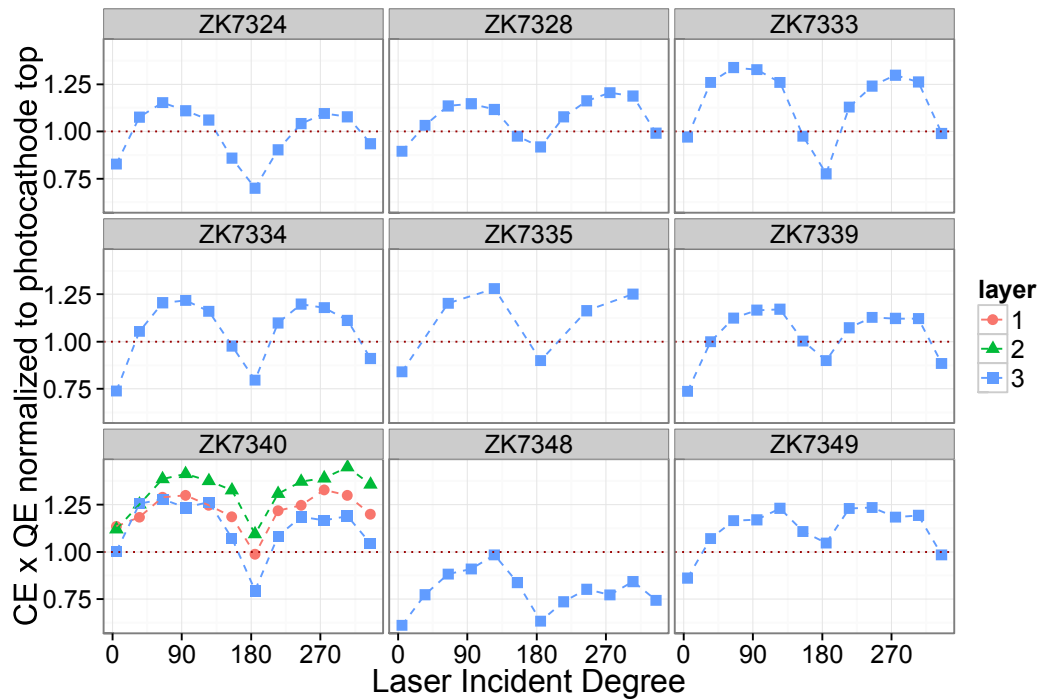


Figure 5: Variation of collection and quantum efficiencies for 9 PMTs. ZK73xx are the serial numbers of the PMTs. Other properties of the figure are the same as Fig. 3b.

Note that the charge presented in Fig. 4 is gain  $\times$  CE  $\times$  QE. Figure 5 shows CE  $\times$  QE, the quotient of charge and gain for 9 PMTs in this production batch.

In Fig. 5, except ZK7340, only Layer 3 was used because it was the most relevant to our purpose being nearest to the detector surface. Keeping in mind that  $360^\circ$  is the same as  $0^\circ$  in the plot, the trend of the variation is symmetric between  $180^\circ$  and  $0^\circ$ . In Fig. 5, ZK7348 has a lower relative CE  $\times$  QE in Layer 3 but with a similar shape of variation. It could be an artifact from variability of laser intensity. Otherwise the PMTs in this batch behaved similarly.

### 3.4. Cryogenic Performance and Material Screening

Cryogenic performance of the PMTs was evaluated. A cooling chamber with liquid  $N_2$  was used. Relaxation of gain and dependence on temperature were observed. Dark rates decreased at low temperature, as expected.

The PMTs were confirmed to be stable in liquid xenon for 1 month, during which no discharge were found.

PMT raw material screening are carried out jointly by the XMASS collaboration and Hamamatsu Photonics Inc. PMT parts before assembly are being screened for RI with HPGe detectors. The design of XMASS-1.5 requires a reduction of RI contamination down to 10 % of the present PMT R10789. The latter has  $0.76 \pm 0.24$  mBq  $^{238}\text{U}$ ,  $1.2 \pm 0.3$  mBq  $^{232}\text{Th}$ ,  $2.9 \pm 0.2$  mBq  $^{60}\text{Co}$  and  $9.1 \pm 2.2$  mBq  $^{40}\text{K}$ .

## 4. Summary

XMASS-1.5 is the next step of the running XMASS-I experiment, scaling up fiducial mass 10 times to 1 t. Measures to counteract background have been developed to reflect our experience with the running detector. The central improvement is the new R13111 PMT with a dome-

shaped photocathode to detect nearby surface radioactivity. A batch of R13111 has been tested in the laboratory. The result met our expectation and showed the feasibility of XMASS-1.5. Further material screen and mass production are scheduled.

### Acknowledgments

The laboratory experiments have been carried out in collaboration with M. Kobayashi, N. Oka, M. Yamashita and B. S. Yang. The XMASS project is supported by the Japanese Ministry of Education, Culture, Sports, Science and Technology, Grant-in-Aid for Scientific Research, JSPS KAKENHI Grant Number, 19GS0204, 26104004.

### Reference

- [1] Aprile E *et al* (Xenon 100 Collaboration) 2012 *Astroparticle Physics* **35** 573
- [2] Auger M *et al* (EXO Collaboration) 2012 *J. Inst.* **7** P05010
- [3] Akerib D S *et al* (LUX Collaboration) 2013 *Nucl. Instr. Meth. Phys. Res. A* **704** 111
- [4] Cao X *et al* (PandaX Collaboration) 2014 *Sci. China Phys. Mech. Astron.* **57** 1476
- [5] Suzuki Y *Preprint* arXiv:hep-ph/0008296
- [6] Abe K *et al* (XMASS Collaboration) 2013 *Nucl. Instr. Meth. Phys. Res. A* **716** 78
- [7] Abe K *et al* (XMASS Collaboration) 2013 *Phys. Lett. B* **719** 78
- [8] Abe K *et al* (XMASS Collaboration) 2014 *Phys. Rev. Lett.* **113** 121301
- [9] Uchida H *et al* (XMASS Collaboration) 2014 *Prog. Theor. Exp. Phys.* **2014** 063C01
- [10] Abe K *et al* (XMASS Collaboration) 2015 *Preprint* **1511.04807**
- [11] Abe K *et al* (XMASS Collaboration) 2013 *Phys. Lett. B* **724** 46
- [12] Abe K, *et al* (XMASS Collaboration) 2015 *Preprint* arXiv:1510.00754